Heat current flows across an interface in two-dimensional lattices

Yanjiang Guo (郭彦江) and Lei Wang (王雷)*

Department of Physics and Beijing Key Laboratory of Opto-electronic Functional Materials and Micro-nano Devices, Renmin University of China, Beijing 100872, People's Republic of China

(Received 29 December 2020; revised 28 March 2021; accepted 30 April 2021; published 28 May 2021)

Heat current J that flows through a few typical two-dimensional nonlinear lattices is systematically studied. Each lattice consists of two identical segments that are coupled by an interface with strength $k_{\rm int}$. It is found that the two-universality-class scenario that is revealed in one-dimensional systems is still valid in the two-dimensional systems. Namely, J may follow $k_{\rm int}$ in two entirely different ways, depending on whether or not the interface potential energy decays to zero. We also study the dependence of J on lattice width N_Y and transverse interaction strength k_Y. Universal power-law decay or divergence is observed. Finally, we check the equipartition theorem in the systems since it is the basis of all our theoretical analyses. Surprisingly, it holds perfectly even at the interface where there is a finite temperature jump, which makes the system far from equilibrium. However, the equipartition of potential energy, which is observed in one-dimensional systems, is no longer satisfied due to the interaction between different dimensions.

DOI: 10.1103/PhysRevE.103.052141

I. INTRODUCTION

Due to the major importance in fundamental physics as well as the apparent value in practice, heat conduction in nanoscale systems has attracted rapidly growing interest [1,2]. The dimension of those microscopic systems is commonly a key factor for thermal transport. There is consensus that heat conductivity κ generally displays a power-law divergence with the system size in one-dimensional (1D) momentum-conserving systems [3], while in 2D systems the divergence is logarithmic [4] and in 3D systems κ converges [5,6]. The dimensional crossover has also been observed both numerically [7,8] and experimentally [9,10]. Some current progress in this field can be found in, for example, comprehensive reviews in [11,12]. Based on the idea that the local heat current is determined not only by the local temperature gradient but by nonlocal ones in other parts of a system as well, a new framework for the study of anomalous transport has emerged very recently, in which the conventional equation of heat conduction is replaced by a spatially nonlocal one [13–15].

In regard to application, much attention has been paid recently to phononics, a new science and engineering of managing heat flow and processing information with heat. Thermal counterparts of many electric devices have been worked out, e.g., thermal diodes that rectify heat current and thermal transistors that switch and modulate heat current [16]. There are two commonly applied mechanisms that can induce a thermal rectifying effect [17]. One relies on the match or mismatch of the phonon spectra at an interface [18,19] and the other relies on the different temperature dependence of heat conductivity of bulk materials [20,21]. The former is normally much more efficient. The case is quite similar for negative differential thermal resistance, the basis of thermal transistors [22]. It is commonly much more easily realized by interface thermal resistance [23].

Besides the large number of theoretical studies, the rapid development of nanoscale technology has also enabled us to measure heat conduction in nanoscale materials experimentally, particularly in various 2D materials such as graphene [24,25] and 2D MoS_2 [26,27]. The key role of the grain interfaces in polycrystalline hexagonal boron nitride thin films has also been studied both experimentally and numerically [28]. Some related progress has been reviewed in a recent colloquium [29].

We have studied the scaling property of the heat-current flows across a one-dimensional weak interface [30] and revealed two universal classes of asymptotic behavior of the heat current j in the small interface interaction strength $k_{\rm int}$ limit. If the interface potential energy $h_{\rm int}$ decays with $k_{\rm int}$ linearly, then the system belongs to class 1, in which $j \sim k_{\rm int}^2$. This was previously expected [31]. However, if such a condition is not satisfied and $h_{\rm int}$ approaches a nonzero constant, then the system belongs to class 2, in which the mean square relative displacement between interface particles $\Delta_{\rm int}^2 \sim k_{\rm int}^{-\alpha}$ and $j \sim k_{\rm int}^{\alpha}$, where α depends on the detail of the interface interaction and commonly $\alpha \in (0, 1]$.

In this paper we study the scaling properties of 2D interface heat conduction, including not only the dependence on the interface strength, but also that on the lattice width and transverse interaction strength. Since the dimension of materials is generally crucial in microscopic heat conduction, more interesting features are naturally expected. The basis of our theoretical analysis, the equipartition theorem, will be carefully checked, in particular at the interface where there is a finite temperature jump, which makes the state far from equilibrium.

*phywanglei@ruc.edu.cn

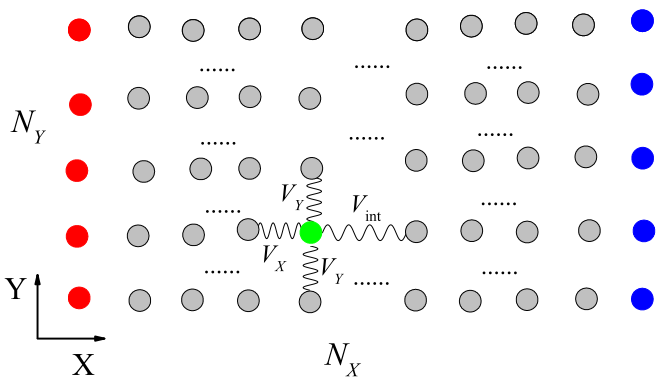

FIG. 1. Configuration of the two-dimensional lattice with N_X columns and N_Y layers. Particles at the left and right ends (colored in red and blue) are coupled to heat baths with high and low temperatures. Thus heat flows from left to right in the X direction.

The paper is organized as follows. The 2D lattices and interface interactions are introduced in Sec. II. The results of detailed numerical simulation and the corresponding theoretical analysis are presented in Sec. III. The validity of the equipartition theorem will be checked in Sec. IV. A summary and discussion are provided in Sec. V.

II. LATTICE MODELS AND INTERFACE INTERACTIONS

The system we study is a 2D lattice that consists of two identical segments that are coupled by an interface with interaction $V_{\rm int}$. In each segment, particles are coupled with their nearest neighbors in the X and Y directions with interactions V_X and V_Y, respectively. The whole system consists of N_X columns and N_Y layers particles. Its configuration is presented in Fig. 1. The Hamiltonian of the system is given by

$$\begin{aligned} H &= H_L + H_{\rm int} + H_R \\ &= \sum_{i=1}^{N_X/2}\sum_{j=1}^{N_Y}\left[\frac{m_{i,j}v_{i,j}^2}{2} + U(u_{i,j}) + V_X(u_{i,j}-u_{i-1,j}) + V_Y(u_{i,j}-u_{i,j-1})\right] + \sum_{j=1}^{N_Y} V_{\rm int}(u_{N_X/2+1,j}-u_{N_X/2,j}) \\ &\quad + \sum_{i=N_X/2+1}^{N_X}\sum_{j=1}^{N_Y}\left[\frac{m_{i,j}v_{i,j}^2}{2} + U(u_{i,j}) + V_X(u_{i+1,j}-u_{i,j}) + V_Y(u_{i,j}-u_{i,j-1})\right]. \end{aligned} \tag{1}$$

Unless otherwise stated in Sec. IV B, free and periodic boundary conditions (BCs) are applied in the X and Y directions, respectively, i.e.,

$$u_{0,j} = u_{1,j}, \quad u_{N_X+1,j} = u_{N_X,j},$$
$$u_{i,0} = u_{i,N_Y}, \quad u_{i,N_Y+1} = u_{i,1}.$$

Two representative lattices will be studied: (i) the ϕ^4 lattice[1] [32] with $V_X(u) = k_X\frac{1}{4}u^4$, $V_Y(u) = k_Y\frac{1}{4}u^4$, and $U(u) = \frac{1}{4}u^4$ and (ii) the purely quartic (PQ) lattice with $V_X(u) = k_X\frac{1}{4}u^4$, $V_Y(u) = k_Y\frac{1}{4}u^4$, and $U(u) = 0$. Throughout this paper, k_X is always fixed to 1 and k_Y is also fixed to 1 unless otherwise stated in Sec. III B 3.

Similar to the 1D cases, a detailed type of interaction does play an important role in determining the decay properties of the heat current J even in the small interface strength $k_{\rm int}$ limit. We study three representative types of interactions, i.e., (i) the nonlinear PQ interface interaction where $V_{\rm int}(u) = k_{\rm int}\frac{1}{4}u^4$, (ii) the linear interface interaction where $V_{\rm int}(u) = k_{\rm int}\frac{1}{2}u^2$, and (iii) the rotator interface interaction where $V_{\rm int}(u) = k_{\rm int}[1-\cos(u)]$.

III. NUMERICAL SIMULATIONS

To keep the system in a nonequilibrium stationary state, Langevin heat baths with slightly different temperatures $T_L = 1.1$ and $T_R = 0.9$ are attached to the left and right ends (the particles in the first and the N_Xth columns). The dynamics of the system is governed by the Langevin equation

$$\ddot{u}_{i,j} = -\frac{\partial H}{\partial u_{i,j}} + \delta_{i,1}(-\gamma\dot{u}_{i,j} + \xi_j) + \delta_{i,N_X}(-\gamma\dot{u}_{i,j} + \eta_j), \tag{2}$$

where $\langle\xi_j(t)\rangle = \langle\eta_j(t)\rangle = 0$, $\langle\xi_j(t_1)\eta_k(t_2)\rangle = 0$, $\langle\xi_{j_1}(t_1)\xi_{j_2}(t_2)\rangle = 2\gamma T_L\delta_{j_1,j_2}\delta(t_2-t_1)$, and $\langle\eta_{j_1}(t_1)\eta_{j_2}(t_2)\rangle = 2\gamma T_R\delta_{j_1,j_2}\delta(t_2-t_1)$. The damping coefficient γ of the heat baths is set equal to 1. A fifth-order Runge-Kutta algorithm [33] with time step size 0.01, which provides high cost-effectiveness and sufficient accuracy, is applied for the numerical calculation. For simplicity, the lengths of the left and the right segments are fixed to $N_X/2$ and the mass of all the particles is set to unity. In order to concentrate on the interface effects, N_X is fixed to a short length $N_X = 16$. We also check that a longer choice of N_X, say, 32, does not change the results. This choice confirms that the bulk resistance is negligible but the effects from the boundaries or heat baths vanish.

In the nonequilibrium stationary state, a heat current J flows from left to right,

$$J \equiv \sum_{j=1}^{N_Y}\left\langle\frac{\partial V_X(u_{i+1,j}-u_{i,j})}{\partial u_{i,j}}\dot{u}_{i,j}\right\rangle. \tag{3}$$

The heat current J is a constant in the X direction, i.e., label i independent. Its per-layer average $j \equiv \frac{J}{N_Y}$. In our previous study [30], we revealed that the mean square relative

[1]Normally, the interparticle interaction of the ϕ^4 lattice is linear and thus our model can be regarded as a ϕ^4-like one. In this paper we still call it the ϕ^4 lattice for simplicity.

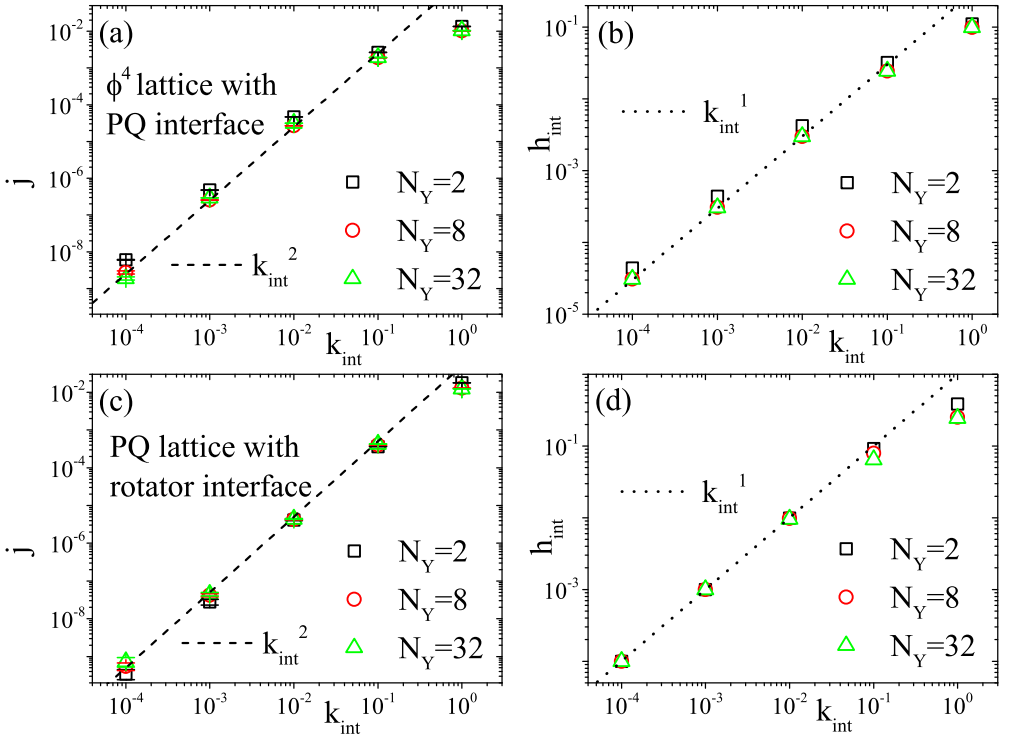

FIG. 2. (a) and (c) Per-layer average heat current j and (b) and (d) per-layer average interface potential energy $h_{\rm int}$ for the ϕ^4 lattice with (a) and (b) the PQ interface and (c) and (d) the PQ lattice with the rotator interface. Here $N_X = 16$ and $N_Y = 2$, 8, and 32. Dashed and dotted lines for $k_{\rm int}^2$ and $k_{\rm int}^1$,respectively, are plotted for reference.

displacement (MSRD) between interface particles

$$\Delta_{\rm int}^2 \equiv \frac{1}{N_Y}\sum_{j=1}^{N_Y}\langle(u_{N_X/2+1,j} - u_{N_X/2,j})^2\rangle, \tag{4}$$

the interface potential energy

$$H_{\rm int} \equiv \sum_{j=1}^{N_Y}\langle V_{\rm int}(u_{N_X/2+1,j} - u_{N_X/2,j})\rangle, \tag{5}$$

and the per-layer average $h_{\rm int} \equiv H_{\rm int}/N_Y$ play key roles in determining the scaling properties, which we will study in depth.

A. Class-1 models

The class-1 models include (a) lattices with a hard on-site potential and (b) lattices with soft interface interactions [30]. Here the words soft and hard mean that $\lim_{u\to\pm\infty} V_{\rm int}(u)$ is finite and divergent, respectively. Correspondingly, we study two typical cases: the ϕ^4 lattice with nonlinear quartic interface interactions and the PQ lattice with rotator interface interactions.

In the former case the probability distribution function of the relative displacement between any pair of interface particles approaches a $k_{\rm int}$-independent asymptotic distribution $P(\Delta u)$ in the small-$k_{\rm int}$ limit, where $\Delta u \equiv u_{N/2+1,j} - u_{N/2,j}$. If we suppose that $V_{\rm int}(\Delta u) = k_{\rm int} f(\Delta u)$, the potential energy between this pair of particles equals $\int_{-\infty}^{-\infty} V_{\rm int}(\Delta u)P(\Delta u)d\Delta u = k_{\rm int}\int_{-\infty}^{-\infty} f(\Delta u)P(\Delta u)d\Delta u$. It decays with $k_{\rm int}$ linearly since the last integral is finite, nonzero, and $k_{\rm int}$ independent. In the latter case, $f(\Delta u)$ is finite and with period 2π. In the small-$k_{\rm int}$ limit, $P(\{\Delta x\})$ approaches a $k_{\rm int}$-independent asymptotic distribution, where $\{u\} \equiv u - [\frac{u}{2\pi}]2\pi$, with $[u]$ denoting the largest integer that is no greater than u. Therefore, the average potential energy equals $\int_0^{2\pi} V_{\rm int}(\{\Delta u\})P(\{\Delta u\})d\{\Delta u\} = k_{\rm int}\int_0^{2\pi} f(\{\Delta u\})P(\{\Delta u\})d\{\Delta u\}$. For the same reason it again decays linearly with $k_{\rm int}$.

Since $h_{\rm int}$ is proportional to $k_{\rm int}$, it is easy to understand that the proof in Ref. [31] remains valid for the 2D models. Therefore, in both cases the conclusion that the heat current decays as $k_{\rm int}^2$ holds. In Fig. 2 the per-layer average heat current j and the per-layer average interface potential energy $h_{\rm int}$ are plotted for the two cases. All the above expectations are confirmed.

B. Class-2 models

In this class the lattices are momentum conserving and the interface interactions are hard. The case is much more realistic since most of the 2D nanoscale materials for heat conduction measurement in real experiments are suspended [10,34]. To concentrate the study, we consider PQ lattices, and the interface interactions are linear or PQ only. The main results are plotted in Fig. 3.

1. Role of the interface interaction

First, we study the role of the interface interactions. We see in Figs. 3(b) and 3(e) that $H_{\rm int}$ approaches $k_{\rm int}$ independent constants $\frac{T}{2}$ and $\frac{T}{4}$ in the small-$k_{\rm int}$ limit for the linear and

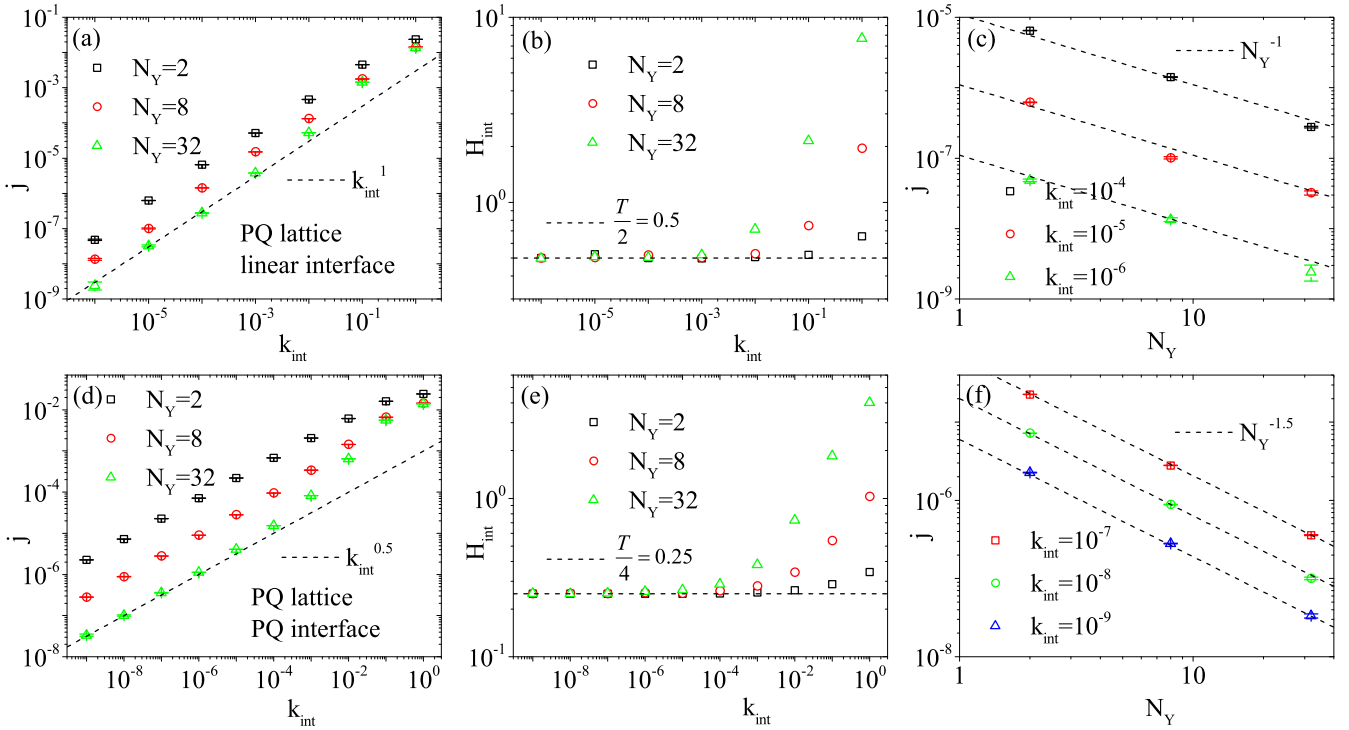

FIG. 3. (a)–(c) PQ lattice with linear interactions and (d)–(f) PQ interface interactions: (a) and (d) average heat current j versus $k_{\rm int}$, (b) and (e) total interface potential energy $H_{\rm int}$ versus $k_{\rm int}$, and (c) and (f) j versus lattice width N_Y.

quartic interfaces, respectively. It was proved in Ref. [30] that if the interface interaction takes the general form $V_{\rm int}(u) = k_{\rm int}\frac{1}{n}u^n$, where n refers to an even integer hereafter, then $j \sim k_{\rm int}^{\alpha}$ and $\Delta_{\rm int}^2 \sim k_{\rm int}^{-\beta}$, where the power exponents $\alpha = \beta = 2/n$. The proof remains valid for the 2D cases since it is dimension independent. Therefore, for the two kinds of interface interactions α should equal 1 and 0.5, respectively. The numerical results shown in Figs. 3(a) and 3(d) strongly confirm this.

2. Role of the lattice width N_Y

Second, we study the role of the lattice width N_Y. Commonly, we expect that the total heat current J is proportional to N_Y; thus j should approach a constant. It is however quite surprisingly that j follows a power-law dependence on N_Y in the small-$k_{\rm int}$ limit, i.e., $j \sim N_Y^{-\nu}$, where $\nu = 1$ and 1.5 for the linear and PQ interface interactions, respectively [see Figs. 3(c) and 3(f)]. This finding implies that in the linear interface case the total heat current J is width N_Y independent and furthermore for the PQ interface J decays with N_Y by $N_Y^{-0.5}$, i.e., the wider the lattice, the smaller the total heat current J.

To explain such a counterintuitive N_Y dependence, we study the N_Y dependence of $H_{\rm int}$. In class-2 models, the total momentum is conserved and the interface interaction is hard. In the small-$k_{\rm int}$ limit, the interface MSRD $\Delta_{\rm int}^2$ approaches infinity by $k_{\rm int}^{-\beta}$, where $\beta = 2/n$, but the MSRD between the same-side particles approaches a temperature-dependent but $k_{\rm int}$-independent finite constant since k_Y is fixed and nonzero. The latter MSRD is thus negligible. All the particles at the left or right side of the interface can be regarded as a single big particle with mass N_Y and the two big particles are connected by an interface interaction with strength $N_Y k_{\rm int}$. In the case that the interface interaction takes the form $V_{\rm int}(u) = k_{\rm int}\frac{1}{n}u^n$, the total interface potential energy

$$H_{\rm int} = \frac{T}{n}, \tag{6}$$

which has been confirmed numerically in Figs. 3(b) and 3(e) for $n = 2$ and 4, respectively. Thus the per-layer average potential energy $h_{\rm int} = \frac{T}{nN_Y}$. Straightforwardly,

$$\Delta_{\rm int}^2 \sim N_Y^{-2/n}, \tag{7}$$

and thus

$$J \sim N_Y^{-(n-2)/n}, \quad j \sim N_Y^{-(2n-2)/n}. \tag{8}$$

These are confirmed in Figs. 3(c) and 3(f) exactly. The counterintuitive N_Y dependence is then explained.

For class-1 models, either $\Delta_{\rm int}^2$ approaches a nonzero N_Y-independent constant or the interface interactions are soft. As a consequence, it is not $H_{\rm int}$ but its per-layer average $h_{\rm int}$ that becomes N_Y independent [see Figs. 2(b) and 2(d)]. In such cases j will not follow the power-law decay but approach a nonzero N_Y-independent constant.

3. Role of the interlayer interaction strength k_Y

The interactions in the transverse Y direction also play an important role, although the heat conduction is in the X direction. It can be qualitatively understood that the interlayer interactions bind the particles together and thus they cannot easily vibrate and carry heat. A well known fact is that the heat conductivity κ diverges only logarithmically with length L for 2D momentum-conserving systems [4], while it displays

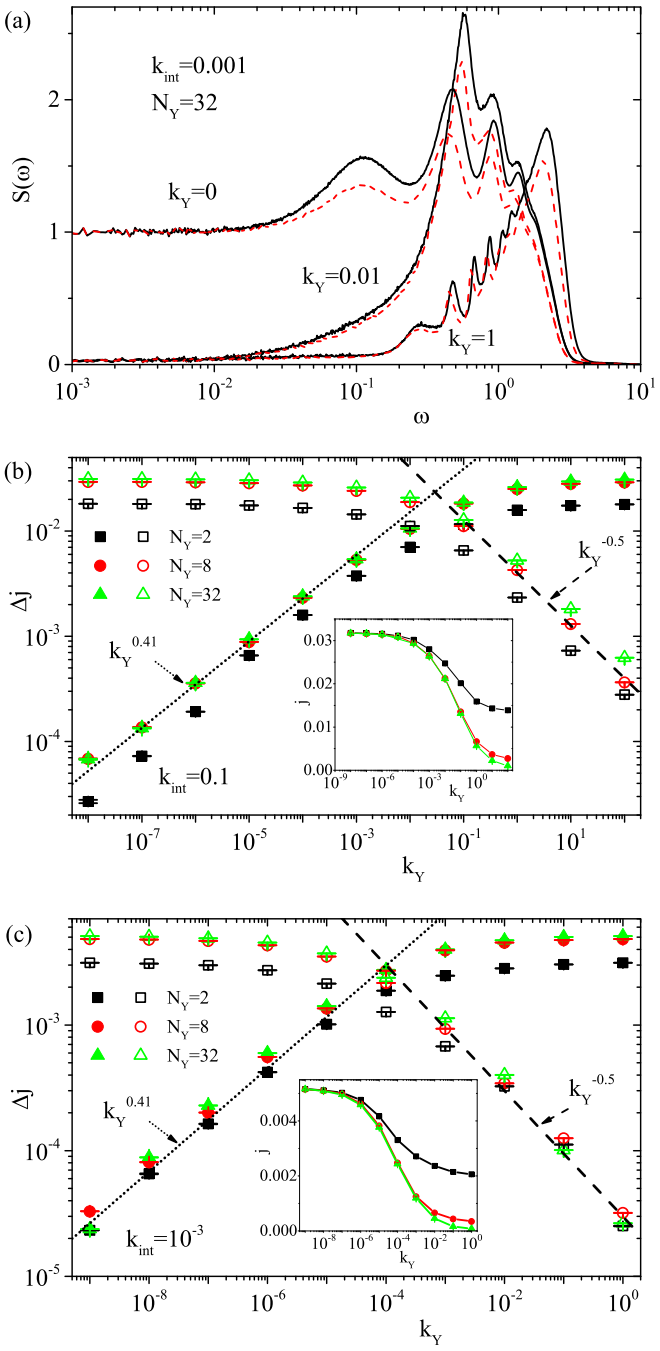

FIG. 4. PQ lattice with the PQ interface. (a) Power spectra $S(\omega)$ of the particles on the left (black solid line) and right (red dashed line) sides of the interface. The three groups from the top down are for $k_Y = 0$, 0.01, and 1, respectively. Those for the left and right particles are slightly different, mainly due to their slightly different temperatures. Also shown are Δj_0 (closed symbols) and Δj_∞ (open symbols) versus k_Y for (b) $k_{\rm int} = 0.1$ and (c) $k_{\rm int} = 10^{-3}$. Dotted lines and dashed lines for $k_Y^{0.41}$ and $k_Y^{-0.5}$, respectively, are plotted for reference. The insets show j versus k_Y.

a power-law divergence with L in 1D systems, which can be regarded as the $k_Y \to 0$ limit of the 2D systems. To present the picture more clearly, we plot the power spectra $S(\omega)$ of the interface particles in Fig. 4(a). Here $S(\omega) \equiv \int R(\tau) e^{i\omega\tau} d\tau$, where $R(\tau)$ refers to the autocorrelation function of the velocity of the particle. We see that even very weak interlayer interactions (say, $k_Y = 0.01$) can largely reduce the power in low-frequency modes, which carry heat much more efficiently than high-frequency modes do.

In contrast to some existing studies on the details of the transverse interactions [35], we are interested more in the general asymptotic ($k_Y \to 0$ and $k_Y \to \infty$) properties. Thus we focus on the PQ lattice with a PQ interface only. The average heat current j versus k_Y for various $k_{\rm int}$ and lattice widths $N_Y = 2$, 8, and 32 is plotted in the insets of Figs. 4(b) and 4(c). For a given value of $k_{\rm int}$ and fixed N_Y, j decreases gradually with k_Y.

In the small- and large-k_Y limits, j approaches $j_0 \equiv \lim_{k_Y \to 0} j$ and $j_\infty \equiv \lim_{k_Y \to \infty} j$, respectively. In the former case the 2D lattice reduces to N_Y separated 1D lattices. Therefore, the average current j_0 is N_Y independent. In contrast, in the latter case the lattice approaches a single 1D lattice in which many quantities, including the mass of particles, the interaction strength in the X direction k_X, the interface interaction strength $k_{\rm int}$, and the heat bath damping coefficients γ, are enlarged N_Y times. Therefore, j_∞ is N_Y dependent. Both values j_0 and j_∞ can be obtained simply by simulating the corresponding 1D lattices.

In order to study the way that the heat currents approach the two limits, we calculate the residuals $\Delta j_0 \equiv j_0 - j$ and $\Delta j_\infty \equiv j - j_\infty$. Plots of Δj_0 and Δj_∞ versus k_Y for various N_Y and $k_{\rm int}$ are shown in Figs. 4(b) and 4(c). Both quantities follow power-law decays very well, i.e.,

$$\Delta j_0 \sim k_Y^{\alpha_0}, \quad \Delta j_\infty \sim k_Y^{-\alpha_\infty}.$$

The two power exponents α_0 and α_∞ are approximately 0.41 and 0.5, respectively. They are basically N_Y and $k_{\rm int}$ independent. We naturally expect that the power exponents remain valid also in the homogeneous case, i.e., $k_{\rm int} = 1$. However, to obtain the value of α_∞ with satisfactory accuracy we need to extend the simulation to even larger values of k_Y, which induces much difficulty in the numerical work. Further studies need to be done to understand the universality of the two power exponents analytically.

IV. THEORETICAL ANALYSES

A. Equipartition theorem at the interface

Since most of the analysis in this paper relies on the equipartition theorem, here we check its validity in our systems, in particular at the interface.

For a classical Hamiltonian system in an equilibrium state with temperature T, equipartition is commonly expected [36], i.e.,

$$T = \left\langle \xi \frac{\partial H}{\partial \xi} \right\rangle, \tag{9}$$

where ξ is any canonical coordinate of the system. For a system in a nonequilibrium state, if the local thermal equilibrium (LTE) holds, i.e., each small portion of the system can still be described by the laws of thermal equilibrium, then

$$T_{i,j} = \left\langle p_{i,j} \frac{\partial H}{\partial p_{i,j}} \right\rangle = \left\langle q_{i,j} \frac{\partial H}{\partial q_{i,j}} \right\rangle \tag{10}$$

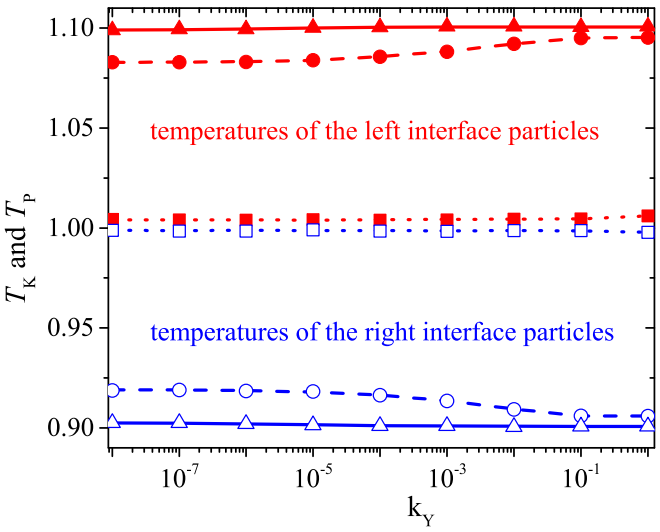

FIG. 5. PQ segments with the PQ interface. Kinetic and potential temperatures at the interface are plotted versus k_Y for various $k_{\rm int}$, with $N_X = 16$ and $N_Y = 8$. The three red upper curves (from the top down) are the kinetic temperatures $T_{K,L}$ of the left interface particles for $k_{\rm int} = 10^{-4}$, 10^{-2}, and 1, respectively. The three blue lower curves (from the bottom up) are those $T_{K,R}$ of the right interface particles for $k_{\rm int} = 10^{-4}$, 10^{-2}, and 1. The symbols are their corresponding potential temperatures $T_{P,L}$ and $T_{P,R}$. Kinetic and potential temperatures always coincide with each other very well.

is expected instead, where $T_{i,j}$ can be regarded as the local location-dependent temperature.

Commonly, LTE is expected only in close-to-equilibrium states. In our systems, however, there exists an interface where the temperature jump is not a small value, and thus the state is in fact far from equilibrium. We will check whether LTE still holds in such a case.

On the left side of the interface, we define

$$T_{K,L} \equiv \frac{1}{N_Y}\sum_{j=1}^{N_Y}\left\langle v_{N_X/2,j}\frac{\partial H}{\partial v_{N_X/2,j}}\right\rangle = \frac{1}{N_Y}\sum_{j=1}^{N_Y}\langle m_{i,j}v_{i,j}^2\rangle, \quad (11)$$

$$T_{P,L} \equiv \frac{1}{N_Y}\sum_{j=1}^{N_Y}\left\langle u_{N_X/2,j}\frac{\partial H}{\partial u_{N_X/2,j}}\right\rangle. \quad (12)$$

Those for the right side, $T_{K,R}$ and $T_{P,R}$, are defined similarly. Here T_K is simply known as the kinetic temperature and T_P is called the potential temperature.

Figure 5 shows $T_{K,L/R}$ and $T_{P,L/R}$ for the 2D PQ lattice with a PQ interface. In all the cases, T_K and T_P always coincide with each other exactly. Although equipartition alone cannot guarantee LTE, we are inclined to believe that even at the interface where the state is far from equilibrium, LTE still holds very well. This is a little unexpected since LTE breaks down in nonstationary anomalous heat diffusion processes in similar systems even though the perturbation is small [37].

B. Equipartition of potential energy

If all the interactions in a lattice take the form $V(u) = k_{X(Y)}\frac{1}{n}u^n$, then Eq. (10) yields

$$\begin{aligned} T_{i,j} &= \langle u_{i,j}\frac{\partial H}{\partial u_{i,j}}\rangle \\ &= k_X\langle u_{i,j}(u_{i,j}-u_{i-1,j})^{n-1}\rangle + k_X\langle u_{i,j}(u_{i,j}-u_{i+1,j})^{n-1}\rangle \\ &\quad + k_Y\langle u_{i,j}(u_{i,j}-u_{i,j-1})^{n-1}\rangle + k_Y\langle u_{i,j}(u_{i,j}-u_{i,j+1})^{n-1}\rangle. \end{aligned} \quad (13)$$

In a homogeneous and rotationally invariant case, it can be written as

$$T_{i,j} = \frac{n}{2}(\langle V_L\rangle + \langle V_R\rangle + \langle V_U\rangle + \langle V_D\rangle), \quad (14)$$

where $\langle V_L\rangle$, $\langle V_R\rangle$, $\langle V_U\rangle$, and $\langle V_D\rangle$ refer to the average potential energies of the interactions that are left, right, up, and down in relation to the particle (i, j). Due to the symmetry, they should all take the identical value $\frac{T_{i,j}}{2n}$.

Now we are interested in whether such an equipartition of potential energy still holds in our system with a weak interface, which is by no means homogeneous and commonly not rotationally invariant. We choose an interface particle, say, the one colored in green in Fig. 1. This time our focus is not the heat current; thus the temperatures of the left and right heat baths are both set to unity. The lattice is thus in an equilibrium state. Furthermore, to increase the symmetry between the X and Y directions, free BCs are applied in both directions.

In Fig. 6 the average potential energies of the interactions to the left of the particle (V_X), at the interface ($V_{\rm int}$), and in the Y direction (V_Y) are plotted. In Fig. 6(a), in which $k_{\rm int} = k_X = 1$, we see the following. (i) When $k_Y = 1$, the lattice reduces to a homogeneous and rotationally invariant one; thus all the potential energies equal $\frac{T}{8}$ and consequently the specific heat c_v equals exactly 0.75, the value of the 1D purely quartic lattice. (ii) In the $k_Y \to 0$ limit, the 2D lattice reduces to several separated 1D homogeneous lattices. All the potentials in the X direction approach $\frac{T}{4}$. As for V_Y, this potential energy approaches a nonzero constant $\frac{T}{4N_X}$, which is proportional to the temperature T but inversely proportional to the lattice length N_X. (iii) In the $k_Y \to \infty$ limit, as we have mentioned, the 2D lattice reduces to a single 1D lattice, in which the particles' mass and all the interaction strength in the X direction are enlarged N_Y times. Therefore, V_X and $V_{\rm int}$ approach $\frac{T}{4N_Y}$ while V_Y approaches $\frac{T}{4}$. Apparently, in both the small- and large-k_Y limits, the right-hand side of Eq. (14) is greater than the temperature T, which implies a local specific heat $c_v > 0.75$ [see the inset of Fig. 6(a)].

The cases are quite similar for $k_{\rm int} = 0.01$, which is shown in Fig. 6(b). However, an apparent difference that can be observed is that since $k_{\rm int} < k_X$, the lattice is no longer homogeneous in the X direction and thus $V_{\rm int}$ is commonly much lower than V_X. The reason is that the interactions in the Y direction confine the motion of the interface particles and thus the MSRD between interface particles $\Delta_{\rm int}^2$ no longer increases with decreasing $k_{\rm int}$ by $k_{\rm int}^{-2/n}$ as it does in the 1D cases. In the small- and large-k_Y limits, the 2D lattice reduces again to several separated 1D lattices and one single 1D lattice, respectively. The above-mentioned effect

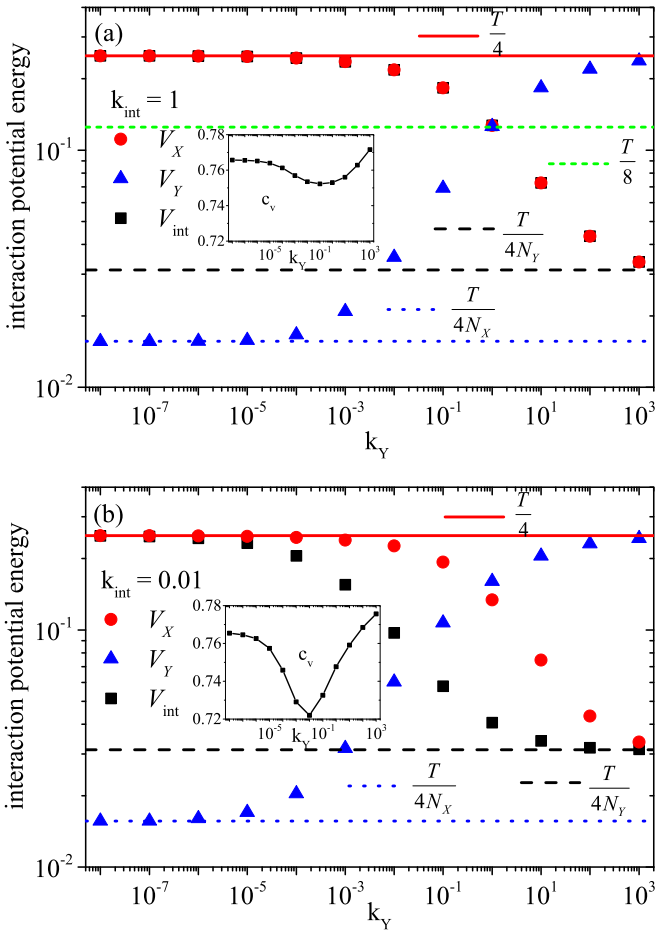

FIG. 6. PQ segments with the PQ interface. Free BCs are applied in both the X and Y directions. Average potential energies V_X (red circles), V_Y (blue triangles), and $V_{\rm int}$ (black squares) of the interactions around an interface particle, say, the green one shown in Fig. 1, are plotted for $N_X = 16$ and $N_Y = 8$, with (a) $k_{\rm int} = 1$, where the lattice is homogeneous in the X direction, and (b) $k_{\rm int} = 0.01$. The horizontal lines indicate the different asymptotic values of the potential energies. The insets show the local specific heat c_v of the interface particles.

vanishes; thus, although $k_{\rm int} \neq k_X$, $V_{\rm int}$ and V_X approach the same values, i.e., $\frac{T}{4}$ for the small-k_Y limit and $\frac{T}{4N_Y}$ for the large-k_Y limit. This confirms our finding in the 1D lattice [30]. Namely, although the 1D lattice is inhomogeneous, the potential energy is still equally shared by different interactions. Very interestingly, although in both the small- and large-k_Y limits the right-hand side of Eq. (14) is again greater than the temperature T, this is not always true. In a quite wide regime of k_Y, the right-hand side is in fact lower than the temperature T, which implies a local specific heat c_v that is even lower than 0.75 [see the inset of Fig. 6(b)]. Basically but not exactly, the more homogeneous the lattice, the lower the specific heat c_v.

Without the equipartition of potential energy, the detailed value of the interface potential energy $H_{\rm int}$ cannot be obtained analytically for a general value of $k_{\rm int}$. However, in the low-$k_{\rm int}$ limit $H_{\rm int}$ still approaches a $k_{\rm int}$-independent constant [see Figs. 3(b) and 3(e)]. That is why the $k_{\rm int}$ dependence of the heat current for 1D models remains unchanged for the 2D models.

TABLE I. Power exponents of the dependence on various parameters. Here 0 refers to independent. The interface interaction takes the form $V_{\rm int}(u) = k_{\rm int}\frac{1}{n}u^n$.

Parameter	$\Delta^2_{\rm int}$	$h_{\rm int}$	j	Δj_0	Δj_∞
		Class 1			
$k_{\rm int}$	0	1	2		
N_Y	0	0	0		
k_Y					
		Class 2			
$k_{\rm int}$	$-\frac{2}{n}$	$\frac{2}{n}$	$\frac{2}{n}$		
N_Y	$-\frac{2}{n}$	-1	$-\frac{2n-2}{n}$		
k_Y				0.41	-0.5

V. CONCLUSION

In summary, we have studied systematically heat conduction across an interface that couples two identical 2D nonlinear segments. Similar to the 1D case [30], the interface strength $k_{\rm int}$ dependence of the heat current J in the small-$k_{\rm int}$ limit still belongs to two classes, namely, $J \sim k^2_{\rm int}$ if the interface potential energy $h_{\rm int}$ decays to zero with $k_{\rm int}$ linearly, while $J \sim k^\alpha_{\rm int}$ if $h_{\rm int}$ approaches a nonzero constant and the interface MSRD $\Delta_{\rm int} \sim k^{-\alpha}_{\rm int}$. Next we studied the role of the width N_Y and the strength of the interlayer interaction k_Y, which is different for 2D systems. It is observed that the total current J is not necessarily an increasing function of N_Y. In the small-$k_{\rm int}$ case, J becomes independent of N_Y for the linear interface and more counterintuitively it decays with N_Y by $N_Y^{-0.5}$ for the PQ interface. As for the k_Y dependence, the average current j approaches different values j_0 and j_∞ in the small- and large-k_Y limits, respectively. The residuals $\Delta j_0 \equiv j_0 - j$ and $\Delta j_\infty \equiv j - j_\infty$ both follow power-law decays, i.e., $\Delta j_0 \sim k_Y^{\alpha_0}$ and $\Delta j_\infty \sim k_Y^{-\alpha_\infty}$, where the power exponents α_0 and α_∞ are approximately 0.41 and 0.5, respectively. The above results are summarized in Table I.

Since the theoretical analysis is mainly based on the equipartition theorem, we checked its validity. It was found that although the theorem is commonly expected only in an equilibrium or a close-to-equilibrium state, it does hold perfectly even at the weak interface where there exists a finite temperature jump and thus the state is far from equilibrium. Finally, we checked the partition of the potential energy in the 2D systems. It was observed that, unlike in the corresponding 1D cases where the potential energy is always shared equally in different interactions, due to the interaction between different dimensions, it is no longer shared equally even among interactions in the same direction. Commonly, stronger interactions share more. The local specific heat c_v is no longer a constant either, and normally the more homogeneous the lattice, the lower the c_v.

These studies may have potential applications in nanoscale heat control and management.

ACKNOWLEDGMENTS

This work was supported by the National Natural Science Foundation of China under Grants No. 12075316 and No.

11675262, by Beijing Natural Science Foundation through Grant No. 1192010, and by the Fundamental Research Funds for the Central Universities, and the Research Funds of Renmin University of China Grant No. 21XNLG26. Computational resources were provided by the Physical Laboratory of High Performance Computing at Renmin University of China.

[1] S. Lepri, R. Livi, and A. Politi, Thermal conduction in classical low-dimensional lattices, Phys. Rep. **377**, 1 (2003).
[2] A. Dhar, Heat transport in low-dimensional systems, Adv. Phys. **57**, 457 (2008).
[3] L. Wang and T. Wang, Power-law divergent heat conductivity in one-dimensional momentum-conserving nonlinear lattices, Europhys. Lett. **93**, 54002 (2011).
[4] L. Wang, B. Hu, and B. Li, Logarithmic divergent thermal conductivity in two-dimensional nonlinear lattices, Phys. Rev. E **86**, 040101(R) (2012).
[5] K. Saito and A. Dhar, Heat Conduction in a Three Dimensional Anharmonic Crystal, Phys. Rev. Lett. **104**, 040601 (2010).
[6] L. Wang, D. He, and B. Hu, Heat Conduction in a Three-Dimensional Momentum-Conserving Anharmonic Lattice, Phys. Rev. Lett. **105**, 160601 (2010).
[7] L. Yang, P. Grassberger, and B. Hu, Dimensional crossover of heat conduction in low dimensions, Phys. Rev. E **74**, 062101 (2006).
[8] P. Di Cintio, R. Livi, S. Lepri, and G. Ciraolo, Multiparticle collision simulations of two-dimensional one-component plasmas: Anomalous transport and dimensional crossovers, Phys. Rev. E **95**, 043203 (2017).
[9] S. Ghosh, W. Bao, D. L. Nika, S. Subrina, E. P. Pokatilov, C. N. Lau, and A. A. Balandin, Dimensional crossover of thermal transport in few-layer graphene, Nat. Mater. **9**, 555 (2010).
[10] X. Xu, L. F. C. Pereira, Y. Wang, J. Wu, K. Zhang, X. Zhao, S. Bae, C. T. Bui, R. Xie, J. T. L. Thong, B. H. Hong, K. P. Loh, D. Donadio, B. Li, and B. Ozyilmaz, Length-dependent thermal conductivity in suspended single-layer graphene, Nat. Commun. **5**, 3689 (2014).
[11] *Thermal Transport in Low Dimensions: From Statistical Physics to Nanoscale Heat Transfer*, edited by S. Lepri, Lecture Notes in Physics Vol. 921 (Springer, Berlin, 2016).
[12] G. Benenti, S. Lepri, and R. Livi, Anomalous heat transport in classical many-body systems: Overview and perspectives, Front. Phys. **8**, 292 (2020).
[13] A. Kundu, C. Bernardin, K. Saito, A. Kundu, and A. Dhar, Fractional equation description of an open anomalous heat conduction set-up, J. Stat. Mech (2019) 013205.
[14] A. Dhar, A. Kundu, and A. Kundu, Anomalous heat transport in one dimensional systems: A description using non-local fractional-type diffusion equation, Front. Phys. **7**, 159 (2019).
[15] W. Wang and E. Barkai, Fractional Advection-Diffusion-Asymmetry Equation, Phys. Rev. Lett. **125**, 240606 (2020).
[16] N. Li, J. Ren, L. Wang, G. Zhang, P. Hänggi, and B. Li, *Colloquium*: Phononics: Manipulating heat flow with electronic analogs and beyond, Rev. Mod. Phys. **84**, 1045 (2012).
[17] B. Hu, L. Yang, and Y. Zhang, Asymmetric Heat Conduction in Nonlinear Lattices, Phys. Rev. Lett. **97**, 124302 (2006).
[18] B. Li, L. Wang, and G. Casati, Thermal Diode: Rectification of Heat Flux, Phys. Rev. Lett. **93**, 184301 (2004).
[19] B. Li, J. Lan, and L. Wang, Interface Thermal Resistance between Dissimilar Anharmonic Lattices, Phys. Rev. Lett. **95**, 104302 (2005).
[20] Y. Yang, H. Chen, H. Wang, N. Li, and L. Zhang, Optimal thermal rectification of heterojunctions under Fourier law, Phys. Rev. E **98**, 042131 (2018).
[21] C. Zhang, M. An, Z. Guo, and S. Chen, Perturbation theory of thermal rectification, Phys. Rev. E **102**, 042106 (2020).
[22] B. Li, L. Wang, and G. Casati, Negative differential resistance and thermal transistor, Appl. Phys. Lett. **88**, 143501 (2006).
[23] G. L. Pollack, Kapitza resistance, Rev. Mod. Phys. **41**, 48 (1969).
[24] A. A. Balandin, S. Ghosh, W. Bao, I. Calizo, D. Teweldebrhan, F. Miao, and C. N. Lau, Superior thermal conductivity of single-layer graphene, Nano Lett. **8**, 902 (2008).
[25] S. Chen, Q. Wu, C. Mishra, J. Kang, H. Zhang, K. Cho, W. Cai, A. A. Balandin, and R. S. Ruoff, Thermal conductivity of isotopically modified graphene, Nat. Mater. **11**, 203 (2012).
[26] K. Xu, A. J. Gabourie, A. Hashemi, Z. Fan, N. Wei, A. B. Farimani, H.-P. Komsa, A. V. Krasheninnikov, E. Pop, and T. Ala-Nissila, Thermal transport in MoS_2 from molecular dynamics using different empirical potentials, Phys. Rev. B **99**, 054303 (2019).
[27] S. Sahoo, A. P. S. Gaur, M. Ahmadi, M. J.-F. Guinel, and R. S. Katiyar, Temperature-dependent Raman studies and thermal conductivity of few-layer MoS_2, J. Phys. Chem. C **117**, 9042 (2013).
[28] H. Ying, A. Moore, J. Cui, Y. Liu, D. Li, S. Han, Y. Yao, Z. Wang, L. Wang, and S. Chen, Tailoring the thermal transport properties of monolayer hexagonal boron nitride by grain size engineering, 2D Mater. **7**, 015031 (2020).
[29] X. Gu, Y. Wei, X. Yin, B. Li, and R. Yang, *Colloquium*: Phononic thermal properties of two-dimensional materials, Rev. Mod. Phys. **90**, 041002 (2018).
[30] L. Wang and Y. Guo, Scaling property of the heat-current flows across a weak interface, Phys. Rev. E **98**, 042108 (2018).
[31] D. S. Sato, Pressure-induced recovery of Fourier's law in one-dimensional momentum-conserving systems, Phys. Rev. E **94**, 012115 (2016).
[32] D. Chen, S. Aubry, and G. P. Tsironis, Breather Mobility in Discrete φ^4 Nonlinear Lattices, Phys. Rev. Lett. **77**, 4776 (1996).
[33] M. L. James, G. M. Smith, and J. C. Wolford, *Applied Numerical Methods for Digital Computation* (HarperCollins, New York, 1993).
[34] S. Lee, D. Broido, K. Esfarjani, and G. Chen, Hydrodynamic phonon transport in suspended graphene, Nat. Commun. **6**, 6290 (2015).
[35] R. Su, Z. Yuan, J. Wang, and Z. Zheng, Tunable heat conduction through coupled Fermi-Pasta-Ulam chains, Phys. Rev. E **91**, 012136 (2015).
[36] A. I. Khinchin, *Mathematical Foundations of Statistical Mechanics* (Dover, New York, 1949).
[37] L. Wang, S. Liu, and B. Li, Validity of local thermal equilibrium in anomalous heat diffusion, New J. Phys. **21**, 083019 (2019).